

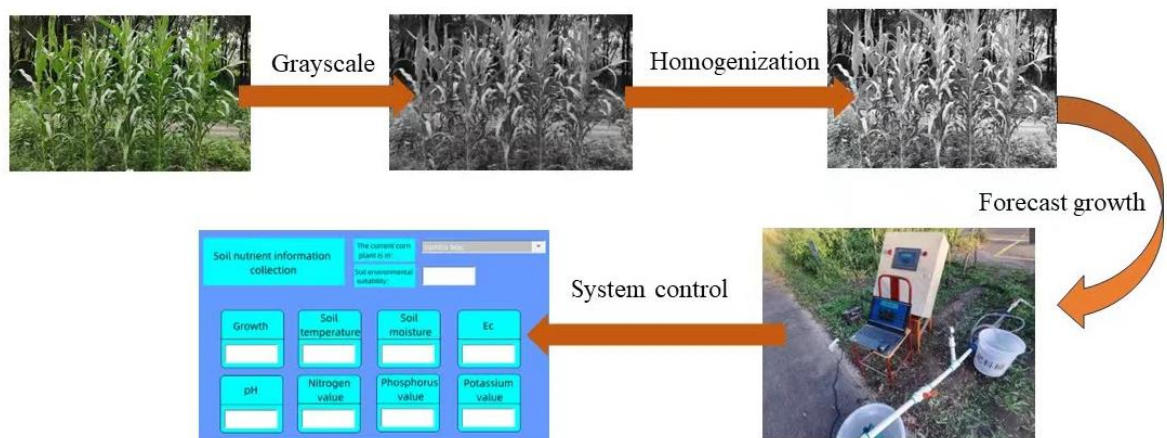
# Maize Plant Growth Period Identification based on MobileNet and Design of Growth Control System

Qiuyan Liang,<sup>a</sup> Xiaoling Zhang,<sup>a</sup> Yiyuan Ge,<sup>a,\*</sup> Tianyue Jiang,<sup>b</sup> and Zihan Zhao<sup>a</sup>

\* Corresponding author: Yiyuan Ge (geyiyuan@qq.com)

DOI: 10.15376/biores.19.3.5450-5466

## GRAPHICAL ABSTRACT



# Maize Plant Growth Period Identification based on MobileNet and Design of Growth Control System

Qiuyan Liang,<sup>a</sup> Xiaoling Zhang,<sup>a</sup> Yiyuan Ge,<sup>a,\*</sup> Tianyue Jiang,<sup>b</sup> and Zihan Zhao<sup>a</sup>

To address the current inefficiencies and subjective nature of manual observation in maize cultivation, with the aim of achieving high efficiency and productivity, this study focused on the DeMaya D3 maize variety. It proposes a maize growth stage recognition method based on the MobileNet model, which is a lightweight convolutional neural network architecture. The method was tested and achieved recognition accuracies of 0.98, 0.96, 0.92, 0.85, and 0.97 for different growth stages, respectively. Additionally, a maize growth prediction model was developed. Based on data collected from experimental plots regarding maize plant height and stem diameter, the Prophet model and an optimized version of the Prophet model were used to forecast maize growth trends. The Prophet model is an open-source tool for time series forecasting. Comparative analysis was conducted between the predictions of the original Prophet model and the optimized version. The relative errors of the Prophet model predictions were 0.85%, 2.11%, and 0.79%, while those of the optimized Prophet model were 0.76%, 0.47%, and 0.71%. Compared to the Prophet model, the optimized model reduced errors by 0.09%, 1.64%, and 0.08%, respectively. The maize plant growth control system was designed to obtain the information through the collection layer. The decision-making layer judged the soil nutrient absorption and growth status. Finally, the management layer controlled water and fertilizer.

DOI: 10.15376/biores.19.3.5450-5466

Keywords: MobileNet; Maize plant; Growth period identification; Control system

Contact information: a: College of Mechanical Engineering Jiamusi University, Jiamusi 154007, China;

b: College of Information and Electronics Technology, Jiamusi University, Jiamusi 154007, China;

\* Corresponding author: Yiyuan Ge (geyiyuan@qq.com)

## INTRODUCTION

As one of the three major crops in China, maize is an important food crop and industrial raw material (Liu *et al.* 2021). Traditional crop growth cycle identification has been mainly based on manual field observation and drawing on historical experience. For example, the seedling stage is centered on nutrient growth. The above-ground part of the plant, leaves and stems, grow slowly, about 2 cm, and is impacted by seedling air permeability and light transmission (Chen *et al.* 2021). The nodulation stage is around 7 to 9 leaves and focuses on water and nutrient supplementation (Huang 2023). The stemming period involves the conversion from nutrient growth to reproductive growth. Female ear development is dominant, and the morphological characteristics of the period show that the top male ears are exposed from the leaf sheaths, focusing on the reasonable control of exuberance (Gu *et al.* 2023). The external characteristics of the milk ripening period are the bottom of the maize plant flowering maize cobs. The perfect ripening stage is the best time to harvest maize, as the plant is full of kernels and dry leaves. Accurate identification

of the growth period of maize not only can scientifically grasp the growth cycle of the plant through morphological changes, reflecting the growth status information, but also it can rely on information technology to improve the field management decision support for farmers. Identification will guide the agricultural activities and realize efficient and high-yield planting. Therefore, it is important to study the growth period recognition of maize plants.

Maize plant growth period recognition research mainly focuses on the training of multi-layer recognition model parameter optimization for supervised learning and image preprocessing image enhancement for migration learning in two forms. The two forms are intended to improve the model performance and enhance the expressive ability of the model to improve the accuracy of image recognition. Zhang *et al.* (2018) proposed a multilevel support vector machine (SVM) modelling method, using the particle swarm optimization (PSO) algorithm to iteratively find the optimal SVM model, select the appropriate kernel function, and construct a maize growth period recognition model. The recognition result was 94.8%. Li *et al.* (2021) proposed a multilevel R-CNN model with supervised learning to classify the growth period recognition study. The sample recognition result was 96%. Xu *et al.* (2021) proposed RAdam optimization of ResNet50 model for identification of key reproductive periods with 97.3% recognition accuracy. Zhao *et al.* (2020) used cascaded convolutional neural grid to improve the Yolov3 model to achieve recognition of targets with 98.1% accuracy. Zheng *et al.* (2022) constructed CustomNet (DenseNet) to a VGG16 multi-model for fertility recognition, respectively and the results showed that the average accuracy of the CustomNet model was 98.6%, which provides a comparable method. Lanlan *et al.* (2022) established a dataset by taking pictures from a drone and applied the Swin Transformer model to classify the different growth stages of maize, with an overall accuracy rate of 98.7%, which can better meet the needs of actual production in farmland. Ma *et al.* (2023) proposed a network model of YOLO v5s-CBD to enhance the image sample data to improve the recognition accuracy and convergence speed of the model. Xu *et al.* (2020) constructed a recognition model based on migration learning, which shortens the convergence time of the model by extracting the key information of the target through the convolutional layer. Zhao *et al.* (2020) constructed the CNN-based image recognition model, divided the training set and dataset, and optimized the parameters of the model by combining with Adam. The data enhancement technique effectively alleviated the problem of overfitting recognition results. Xiong *et al.* (2020) pre-segmented and processed the captured images to remove the redundant background feature information and trained the Mask R-CNN model to classify the pictures. Fan *et al.* (2021) improved the Faster R-CNN model by optimizing the training strategy to distinguish seedlings from weeds, which has applicability and generalization. Wang and Wang (2021) improved the model performance by improving the residual module in the migration learning, enhanced the expressive ability of the model, and provided a reference basis for the identification in the actual agricultural production environment. Ikasari *et al.* (2016) used remote sensing technology to collect images and regularization learning and multi-algorithm fusion to form a multi-layer neural network algorithm to classify the growth stages of rice. The dataset identification accuracy was 70.28%. Gupta *et al.* (2020) built a convolutional neural network to categorize weeds and crops, and the ResNet50 neural network recognized 95.23% of crop classification.

The Demeria D3 maize variety was the research object, focusing on its growth morphology characteristics of each period. The research proposes the recognition method of the critical growth period of maize plants and builds the MobileNet model. Using

Python, it seeks the optimal model parameter to improve the accuracy of the image recognition, and on this basis, through the prediction of the plant height model, it produces the growth trend of the maize plants in each period. The research will allow improved mastery of the growth condition and assist the decision-making of its human intervention.

## EXPERIMENTAL

### Growth Period Identification

The experimental area was planted with maize varieties of Demeria D3. A camera was used to take pictures, as shown in Fig. 1. The design of the recognition model for the growing period mainly consisted of three parts, namely, the model construction of the training set, the model validation of the test set, and the visualization processing of the model results. This process included taking the preprocessed pictures as the input of the MobileNet model, setting up the model parameters, constructing the MobileNet model, and visualizing the output of the model. Visualization processing, due to the PyQT5 library had the advantages of multiple controls. Cross-platform and mature technology, through the Python language call PyQT5 library to design the image interface. The recognition resulted in the output layer of the visualization processing to achieve the image classification of the growth period of maize plants.

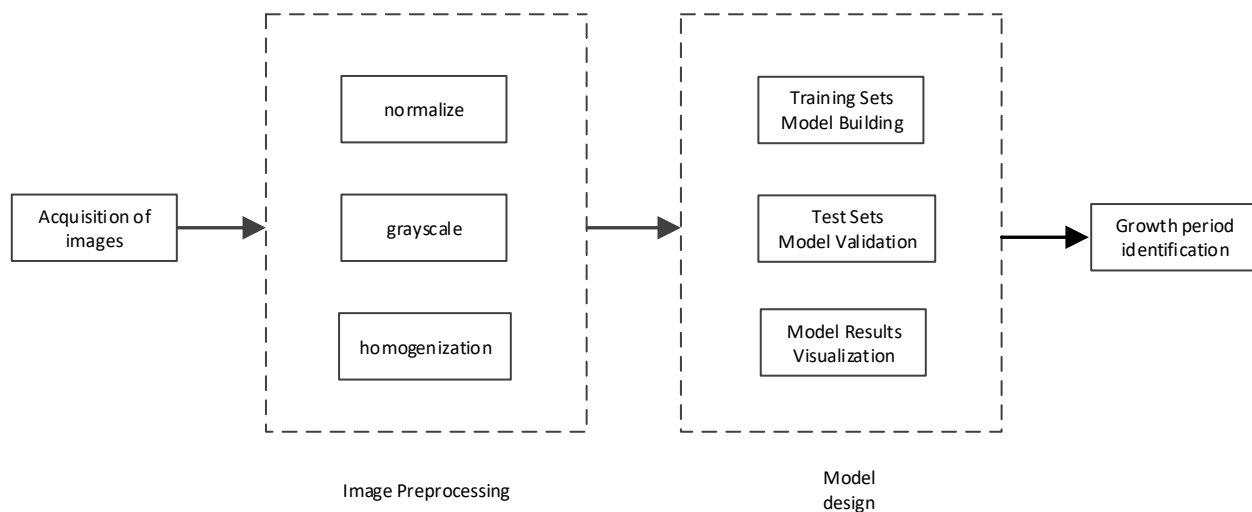


**Fig. 1.** Architecture of maize plants

The growth stages of corn are divided into five phases: seedling stage, jointing stage, tasseling stage, milk ripening stage, and full ripening stage. The seedling stage generally occurs from the 15<sup>th</sup> to the 20<sup>th</sup> day after sowing. During this stage, the soil needs to be kept moist, and adequate amounts of nitrogen, phosphorus, potassium, and other fertilizers should be applied to help the seedlings establish healthy roots and leaves. The jointing stage typically occurs from the 20<sup>th</sup> to the 50<sup>th</sup> day after sowing. During this stage, the soil still needs to be irrigated to maintain moisture, and the application of nitrogen, phosphorus, potassium, and other fertilizers should be increased to meet the needs of plant growth. The tasseling stage generally occurs from the 50<sup>th</sup> to the 64<sup>th</sup> day after sowing. During this stage, potassium and phosphorus fertilizers can be applied in moderate amounts to promote grain formation. The milk ripening stage generally occurs from the 64<sup>th</sup> to the

104<sup>th</sup> day after sowing. During this stage, the demand for water and nutrients by the plants remains high, especially for potassium and phosphorus. The full ripening stage generally occurs from the 104<sup>th</sup> to the 164<sup>th</sup> day after sowing. During this stage, the frequency and amount of irrigation can gradually be reduced, and potassium fertilizer can be applied in moderate amounts to promote grain maturation and improve quality. The DeMaya D3 corn used in this study has a shorter growth cycle and faster growth rate compared to field corn. Under specific growth conditions, it can grow and mature more quickly, which is advantageous for repeated experiments. The HIKVISION MV-CU120-10GC industrial camera was used to capture images of corn plants in this study. This camera has a resolution of 4024 × 3036, a maximum frame rate of 9.7 fps, and a pixel size of 1.85 μm × 1.85 μm. Images of maize plants were captured at regular intervals using a camera to record the growth process of maize at various stages, as shown in Table 1. Maize was planted for a total of 116 days, with 1000 pictures taken in each period, totaling 5000 pictures to construct the maize plant image dataset. The dataset was then divided into training and testing sets in a ratio of 0.8:0.2, with 4000 pictures in the training set and 1000 pictures in the testing set. The pictures in the training set were used to train the MobileNet model, while the pictures in the testing set were used to validate the training effectiveness of the MobileNet model.

**Table 1.** Planting Status of Maize Plants was Recorded

Period	Planting Date	Planting Days
Seedling Stage	From May 26th to June 20th	26
Jointing Stage	From June 21 to July 15	25
Stamen Extraction Stage	From July 16 to August 7	23
Milk Stage	From August 8 to August 27	20
Full Ripe Stage	From August 28 to September 18	22

On-site images of maize plants at seedling, nodulation, and stamen extraction stages were taken to build a dataset with which to perform data preprocessing operations. The integrity and accuracy of the images were retained while serving the purpose of data enhancement of the original images to improve the generalization ability when training the model. Due to variations in shooting angles, the captured images exhibit different orientations, necessitating normalization of the obtained images. Converting the color images to grayscale aids in extracting structural details, better reflecting the target area of the maize plants compared to the original images. Finally, during the process of image equalization, adjustments are made to the pixel grayscale values to find the optimal threshold for maize plant images, thereby reducing issues such as overexposure or underexposure during image acquisition.



**Fig. 2.** Image processing



Through image equalization, the grayscale values of pixels are adjusted, and the cumulative distribution function of the original image is computed to find the optimal threshold for maize plant images. This further extends the dynamic range of pixel grayscale values, ensuring a more uniform distribution of grayscale level distribution values, effectively enhancing the contrast and clarity of maize plant images while minimizing issues arising from excessive brightness or darkness during image capture, as shown in Fig. 2.

### Growth Period Modelling

The MobileNet network model consisted of an input layer, convolutional layer, pooling layer, fully connected layer, and an output layer (Pan 2022). The deep learning framework of PyTorch was written using Python language. The number of training rounds of the model was set through the input layer to read the matrix information in the collected images of maize plants. The convolution layer reduced the dimensionality of the images of maize plants. The pooling layer turned the  $3 \times 3$  depth convolution into a  $1 \times 1$  point-by-point convolution. The local features of the maize plants in each period of growth were extracted through the convolution kernel to realize the classification of the images. Finally, the output layer calculated the error range of the number of iterations in each round to improve the growth period of maize plant recognition accuracy. The model results were obtained by the following equations,

$$W_3 = \frac{W_2 - F}{S} \quad (1)$$

$$W_2 = \frac{W_1 - K + 2P}{S} + 1 \quad (2)$$

$$H_3 = \frac{H_2 - F}{S} + 1 \quad (3)$$

$$H_2 = \frac{H_1 - K + 2P}{S} + 1 \quad (4)$$

$$D_3 = D_2 \quad (5)$$

$$D_2 = D_1 \quad (6)$$

where  $W$  is the width of the image,  $W_1$  is the width of the original image,  $W_2$  is the width of the image after the convolution layer processing,  $W_3$  is the width of the image after the convolution layer processing,  $H$  is the height of the image,  $H_1$  is the width of the original image,  $H_2$  is the width of the image after the convolution layer processing,  $H_3$  is the height of the image after the pooling-layer processing,  $S$  is step,  $F$  is the size of the convolutional kernel,  $K$  is the number of convolutional nuclei, and  $P$  is the zero fill size.

## Plant Height Prediction Modelling and Optimization

The Prophet model was based on the overall trend modelling of arrays with the advantages of fast training speed and high prediction accuracy to predict future trends (Huan *et al.* 2023). The results were the values obtained by adding the trend term, the period term, the holiday term, and the error term. The trend term described the linear or nonlinear changes. The period term described the periodic change rule. The holiday term handled the missing values of the data. The error term made the model prediction results closer to the actual situation. The predicted values of Prophet algorithm can be found through Eq. 7,

$$y(t) = g(t) + s(t) + h(t) + \varepsilon(t) \quad (7)$$

where  $g(t)$  is the trend term,  $s(t)$  is the periodic term,  $h(t)$  is the holiday items,  $\varepsilon(t)$  is the error term, and  $t$  is time.

The logistic curve model is also known as the pear curve model. It is a saturated growth model and its essence is to use the growth rate to reflect the rate of change. It has the advantages of good identification, high prediction accuracy, and strong extension capacity. It can be used to simulate the growth process of the crop growth indicators with the change of the number of days (Cai *et al.* 2020). The parameters of the logistic equation can be obtained from Eq. 8,

$$y(t) = \frac{M}{1 + ae^{-bt}} \quad (8)$$

where  $M$  is the maximum value achievable in the current environment, and  $a$  and  $b$  are undetermined coefficients.

The Numpy library was invoked through Python to read the plant height measurements of maize plants at seedling, nodulation and stamen pulling stages. Daily seasonality trend was changed to establish the plant height prediction model and get the predicted values. The predicted values were substituted into the logistic model, and the parameters of the model were set ( $M$ ,  $a$ , and  $b$ ) to obtain the predicted values of the height of the maize plant and evaluate the performance of the model with the relative error as the evaluation index to complete the model optimization of the Prophet algorithm.

## Maize Plant Growth Control System

Based on the agronomic requirements outlined in "GB1353-2018 Corn Planting Techniques Regulations," the soil nutrient information collection module and the water-fertilizer regulation module were determined, and the overall structural design of the corn plant growth control system was completed (GB 1353-2018). Soil nutrient information is mainly obtained through sensors and uploaded to the PLC. The collected data is displayed on the user interface of the touchscreen, as shown in Fig. 3, showing soil temperature, humidity, pH value, nitrogen, phosphorus, and potassium content of maize plants in the experimental field. Based on the collected data, the system evaluates the suitability of the soil environment and categorizes it into five levels: unsuitable, suitable, moderately suitable, and most suitable. If the assessment indicates unsuitability and the pH is less than 6.5, the plant growth condition is considered as water deficiency; if  $\text{pH} > 8$ , the plant growth condition is considered as nutrient deficiency. Finally, based on the predicted maize plant growth and the assessed soil environment suitability, the system adjusts the ratio and amount of water and fertilizer sprayed. As shown in Fig. 4, the system testing was conducted according to the spacing and ridge spacing of maize planting in the field. During

system operation, water is pumped into the water injection tank, and the pressure gauge on the left measures the inlet pressure. The fertilizer tank sucks in fertilizer through the fertilizer inlet, the Wenchi fertilizer applicator mixes water and fertilizer, and the mixture is then injected into the experimental field. The pressure gauge on the right measures the outlet pressure, and the valve controls the quantity of fertilizer entering and exiting. Each part is connected by PVC pipes.

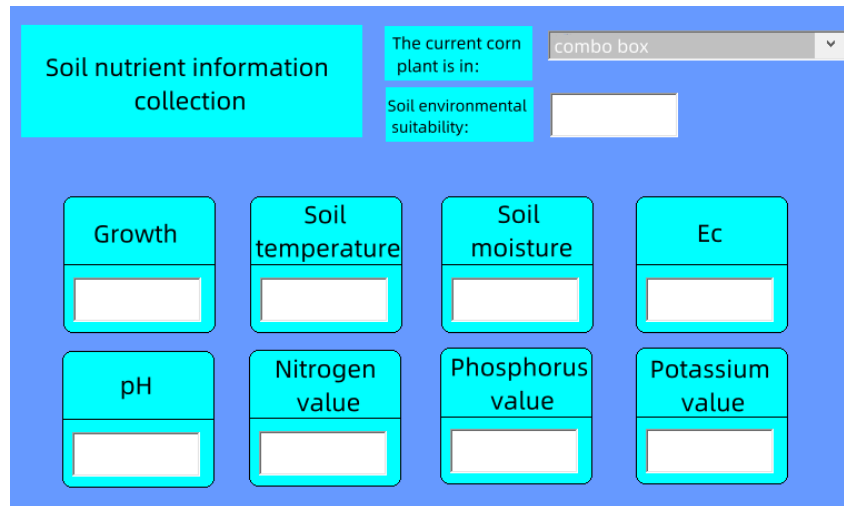


**Fig. 3.** Soil nutrient information collection interface

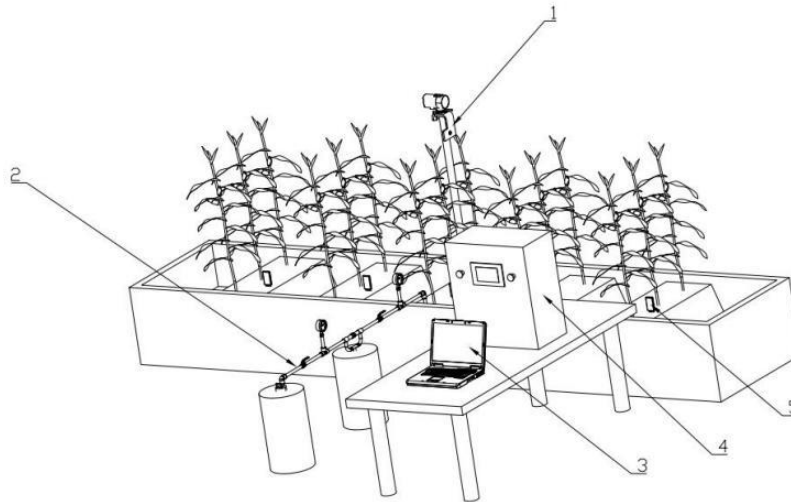


**Fig. 4.** Overall structural design of the system: 1. Image acquisition equipment; 2. Water and fertilizer control device; 3. Remote terminal; 4. Electric control box; 5. Soil sensor

The maize plant growth control system was divided into three parts: acquisition layer, decision-making layer, and management layer. The acquisition layer primarily utilizes sensors and cameras to gather information on soil nitrogen, phosphorus, potassium, temperature, humidity, pH levels, as well as images of maize plants. The decision-making layer assesses the current soil nutrient status, suitability, and the growth condition of maize plants based on the information gathered from the acquisition layer. The management layer mainly carried out water and fertilizer regulation and control, and information management of the remote end through the information judged by the decision-making layer. Considering that the maize plants were planted in outdoor operation, as shown in Fig. 5,



the battery supplies power to the electric control cabinet. The soil status information was monitored through the soil integrated sensor. The pump carried out water and fertilizer regulation through the venturi fertilizer applicator. The WIFI hotspot connected the MCGS touch screen and the remote end, and through the debugging assistant, it realized the cloud login. The remote end built a model through Python to identify the growth period of the maize plants and process the results of growth prediction and display the current operating status of the equipment.

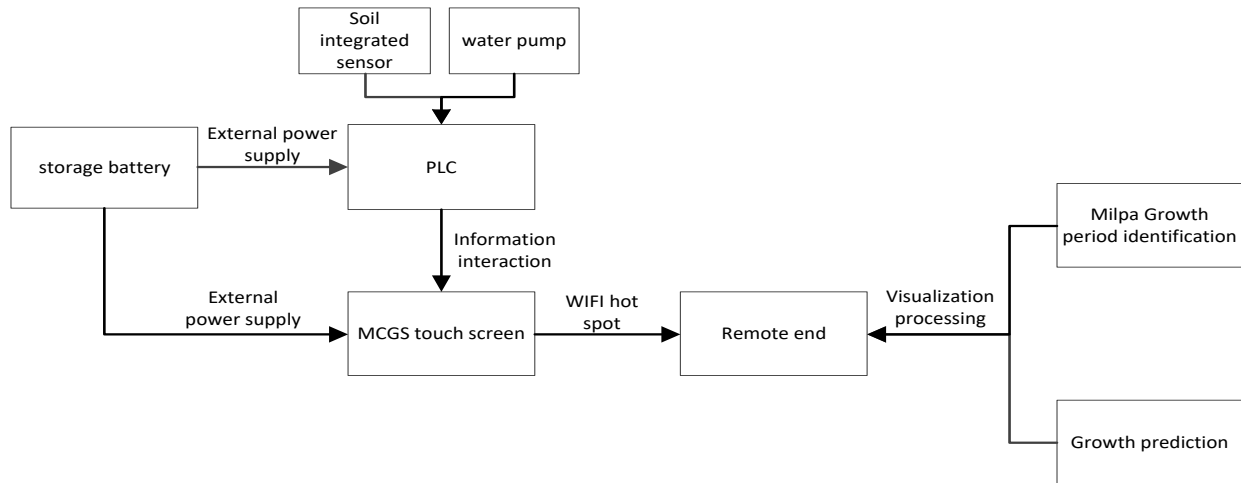


Fig. 5. Overall functional design of the system

### Methods of Regulation of the System

The experimental area was planted with maize, and the camera captured the growth characteristics of maize at different periods. A MobileNet model was built through Python to identify the growth period and was combined with the measured plant height data in the field to judge the growth of the maize plant by the day-by-day growth rate of the plant height. It predicted the trend of the plant height through the optimized model. Maize plant growth period identification and growth prediction were used to better target the critical period of maize for regulation.

As shown in Fig. 6, the water-fertilizer concentration was jointly determined by the amount of fertilizer injected into the pipe and the amount of incoming water in the pipe. It was assumed that during the water-fertilizer mixing process, there is always a flow of water in the pipe and that the concentration of fertilizer is uniformly distributed in all parts of the pipe. Since the volume of the pipe serves as a constant, the pipe can be intercepted and analysed in terms of the unit volume of the pipe.

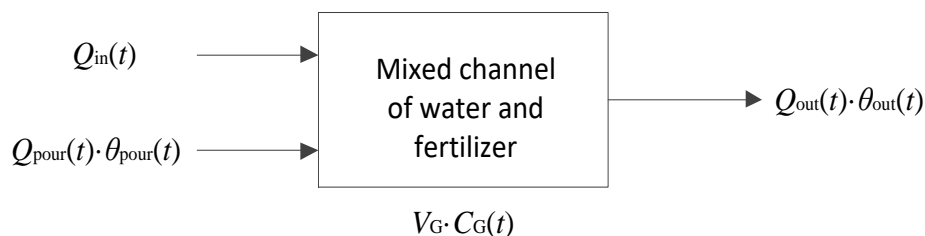


Fig. 6. Water and fertilizer mixed regulation method

According to the conservation of solution volume, the amount of water input into the pipeline plus the amount of fertilizer solution was equal to the amount of mixed solution in the pipeline plus the amount of solution output from the pipeline, which can be obtained from Eq. 9,

$$\int [Q_{\text{pour}}(t) + Q_{\text{in}}(t)] \cdot dt = V_G + \int Q_{\text{out}}(t) \cdot dt \quad (9)$$

where  $Q_{\text{in}}(t)$  is water intake per unit of time ( $\text{m}^3/\text{h}$ ).

Considering the water-fertilizer mixing process, there existed a certain proportional relationship between the concentration of fertilizer injected and the concentration of fertilizer out of the pipe. The concentration of fertilizer injected can be configured in advance, and the amount of fertilizer injected was derived from Eq. 10,

$$Q_{\text{out}}(t) = \frac{\theta_{\text{out}}(t)}{\theta_{\text{out}}(t) - \theta_{\text{in}}(t)} \cdot Q_{\text{in}}(t) \quad (10)$$

General crop fertilizer spraying concentration requirements did not exceed 0.3%, of which urea was between 0.4 to 0.6%. The sensor collects soil nutrient data, and when the collected monitoring data is lower than the demand, the difference between the two is calculated as the amount of fertilizer applied to the crop (Chen 2021). In this case, the specific calculation of fertilizer application time was obtained from Eq. 11 and 12,

$$T_{\text{spread}} = \frac{Q_{\text{fertilizer}} \times 3.6 + T_{\text{water}} \times Q_{\text{in}}}{Q_{\text{pour}}} \quad (11)$$

$$T_{\text{water}} = \frac{Q_{\text{water}} + Q_{\text{max}}}{Q_{\text{overflow}}} \times 3600 \quad (12)$$

where  $T_{\text{spread}}$  is fertilization time (h),  $T_{\text{water}}$  is water supplying time (h),  $Q_{\text{fertilizer}}$  is fertilizer demand ( $\text{m}^3/\text{h}$ ),  $Q_{\text{water}}$  is water supply demand ( $\text{m}^3/\text{h}$ ), and  $Q_{\text{max}}$  is maximum flow ( $\text{m}^3/\text{h}$ ).

## RESULTS

### Analysis of the Effect of Growth Period Identification

As shown in Fig. 7, the preprocessed image was used as input to the MobileNet model. The number of training rounds of the model was 10 rounds. The error was corrected using the Adam optimizer. The error rate of the model in the training set of maize plant growth stage recognition decreased with the number of training rounds, and the maize plant growth stage recognition model was verified by the test set to verify the effectiveness of the model.

The results showed that the maize plant was in the seedling stage, the node pulling stage, and the male-pulling stage. The accuracies of maize plants at seedling, node pulling, staminate pulling, milk ripening and maturity stage were 98%, 96%, 92%, 85%, 97%, respectively.

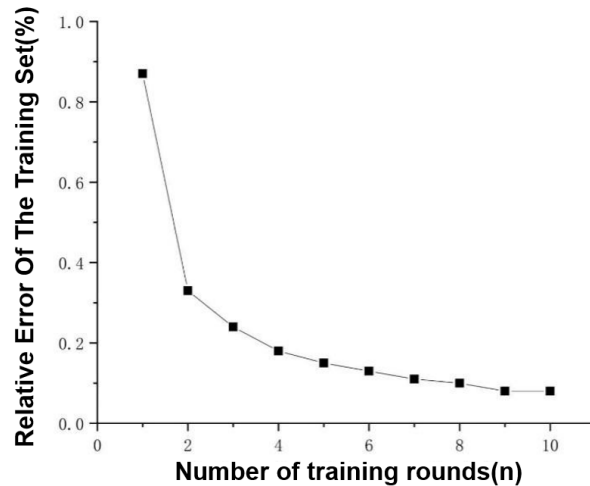


Fig. 7. Growth-term recognition of maize plants

### Analysis of Plant Height Prediction Model Results

Based on the measured data of maize plant height during the seedling stage, jointing stage, and tasseling stage, a maize plant height prediction model was established using the training set, consisting of a Prophet model and an optimized Prophet model coupled with the Logistic model. The predictive performance of the models was verified using the test set. To compare and analyze the actual prediction effect of each model, the relative error was used as the evaluation index, and the smaller values indicated that the prediction value was closer to the value of the test set (Liang *et al.* 2023). The error of the model can be obtained from Eq. 13,

$$\text{error} = \left| \frac{f_i - y_i}{y_i} \right| \times 100\% \tag{13}$$

where  $f_i$  is predicted value and  $y_i$  is trial value.

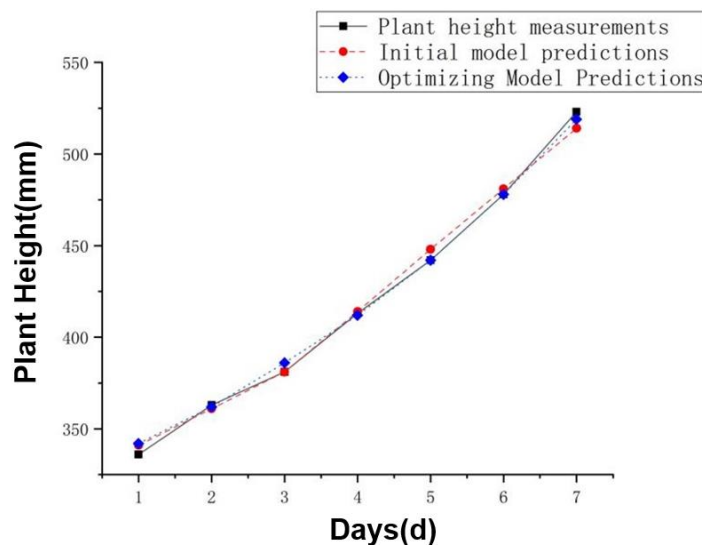
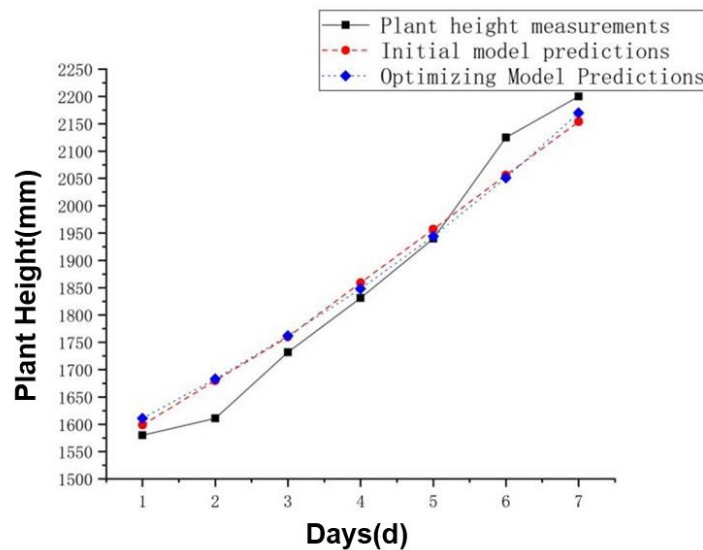


Fig. 8. Prediction of plant height model in maize seedling images

The parameters of Prophet model were set, the growth trend was set as linear, and the seasonal pattern of data series was set as additive as well as the daily trend change being automatically identified. The values of model parameters  $M$ ,  $a$ , and  $b$  of the optimized Prophet model were 14.05, -0.96, and -0.002, respectively, and the effect of predicting the height of seedling maize plants is shown in Fig. 8.

As shown in Fig. 9, compared to the seedling stage, the growth rate of maize plant height was more obvious at the nodulation stage, and the Prophet model parameters were set to keep the same with the seedling stage parameters. The Prophet model was optimized with the value of  $M$  taken as 87.75, the value of  $a$  taken as -0.94, and the value of  $b$  taken as -0.005.



**Fig. 9.** Prediction of plant height model in maize jointing phase images

As shown in Fig. 10, compared with the nodulation stage, the plant height growth rate of maize plants in the period of staminate extraction was relatively slow, and the predicted values of Prophet model were substituted into the logistic model.  $M$  had a value of 289,  $a$  had value of -0.90, and  $b$  had a value of 0.001 to obtain the predicted values of plant height.

Under the PyCharm compilation environment, the plant height prediction models for seedling stage, nodulation stage, and staminate extraction stage were established in Python. The planting date of seedling stage was from May 26 to June 20, with a total of 26 days, and the mean value of plant height was 233 mm. The planting date of nodulation stage was from June 21 to July 15, with a total of 25 days, and the mean value of plant height was 1,194 mm. The planting date of nodulation stage was from July 16 to August 7, with a total of 23 days, and the mean value of plant height was 2,825 mm. The planting date of the stigmatic stage was from July 16 to August 7, with a total of 23 days, and the average value of plant height was 2825 mm. The relative errors of the Prophet model's predicted values were 0.85%, 2.11%, and 0.79%, while those of the Prophet optimization model were 0.76%, 0.47%, and 0.71%, which were reduced by 0.09%, 1.0%, 1.0%, and 1.0%, respectively, compared with those of the Prophet model. reduced by 0.09%, 1.64% as well as 0.08%.

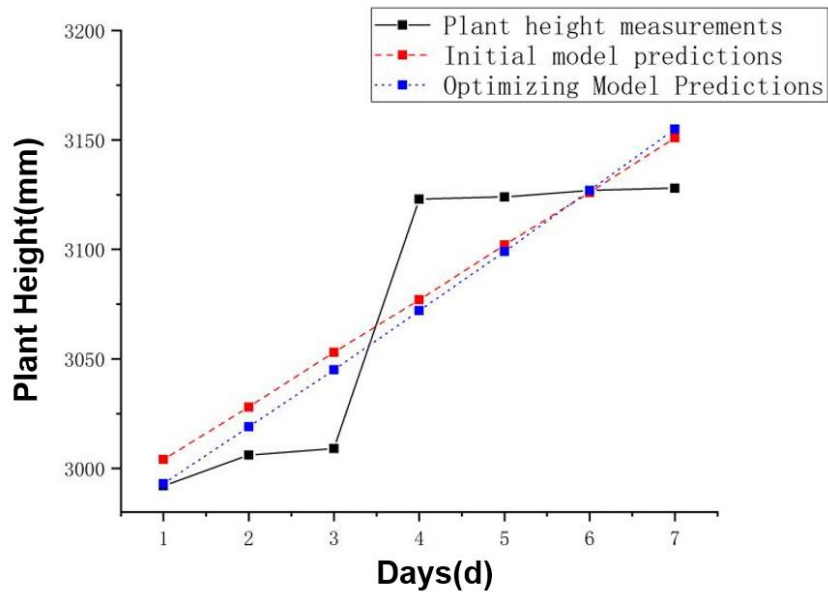


Fig. 10. Prediction of plant height model in maize maturation period Images

Table 2. Evaluation of the Plant-Height Prediction Model

Period Of Growth	Prophet Model Fractional Error	Prophet Optimize the Model Fractional Error
Seedling Stage	0.85	0.76
Shooting Period	2.11	0.47
Tasseling Stage	0.79	0.71

Using McgsPro configuration software, the configuration interface design of soil nutrient information acquisition was carried out. To obtain PLC data, in the equipment window, the driver of Delta PLC was set. Soil temperature, humidity value, pH value and nitrogen, phosphorus and potassium content of maize plants in the experimental field were read through the user window. The suitability of the soil environment was judged by detecting the pH value of the soil, which was divided into five grades of unsuitable, suitable, sub-suitable and the most suitable. If the judgment result was unsuitable and the pH was less than 6.5, the plant growth condition was water shortage, and if the pH was more than 8, the plant growth condition was fertilizer shortage. If  $\text{pH} > 8$ , the plant growth condition was fertilizer deficiency. Water and fertilizer control management was mainly divided into manual mode and automatic mode. The user can switch to choose and control the start and stop of the pump. The system operation indicator showed the current system operation status. Remote end acquisition enabled cloud-based off-site login to view the current operating status of the device. The configuration interface script was designed to display the predicted value of plant height by determining that the maize plant was in a certain lifetime and combining it with the number of days of planting (Fig. 11) by substituting the formula of the prediction model for the plant height of the maize plant into the MCGS screen.





Fig. 11. Commissioning of the maize growth control system

### System Fertilization Performance Analysis

Measurement of the system's fertilizer absorption performance indicators were three types of fertilizer absorption, fertilizer concentration, and fertilizer absorption efficiency (Zhang and Li 2019). The fertilizer absorption  $M$  was used to reflect fertilizer quantity. The fertilizer concentration  $\theta$  was used to reflect the performance of fertilizer suction good or bad, and the fertilizer efficiency  $\eta$  was used to evaluate the comprehensive fertilizer suction performance of fertilizer suction. The higher the efficiency was, the more significant the comprehensive fertilizer suction performance on behalf of the Venturi Fertilizer Apparatus. As shown in Fig. 12, when the inlet pressure of the venturi fertilizer applicator varied within the range of 0.01 to 0.1 MPa, the inlet flow rate ratio increased from 5.8 to 12.1% with the continuous increase of the inlet pressure.

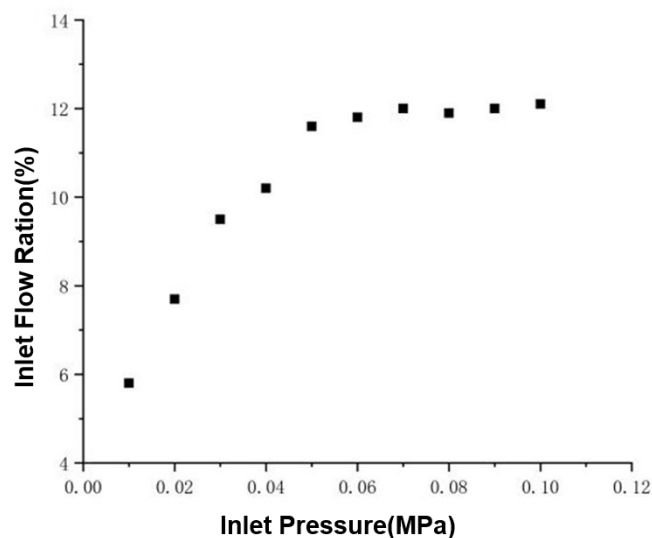


Fig. 12. The relationship between the import flow ratio and the import pressure

The test results showed that with the increase of the inlet pressure, it reached the peak at 0.06 MPa, and the working performance reached the optimal state. The value of the inlet flow rate ratio tended to be in the stable state, and it did not change with the inlet pressure.

As shown in Fig. 13, when the inlet pressure of the venturi fertilizer applicator varied within the range of 0.01 to 0.1 MPa, the trend of the fertilizer concentration was first fast and then slow, and the fertilizer concentration increased from 5.7% to 10.5%. The test results showed that with the increase of the inlet pressure, the upward trend was the largest in 0.04 MPa, at which time the concentration of fertilizer was 9.9%, and the value of the fertilizer concentration tended to be in the stable state and did not change with the inlet pressure changes.

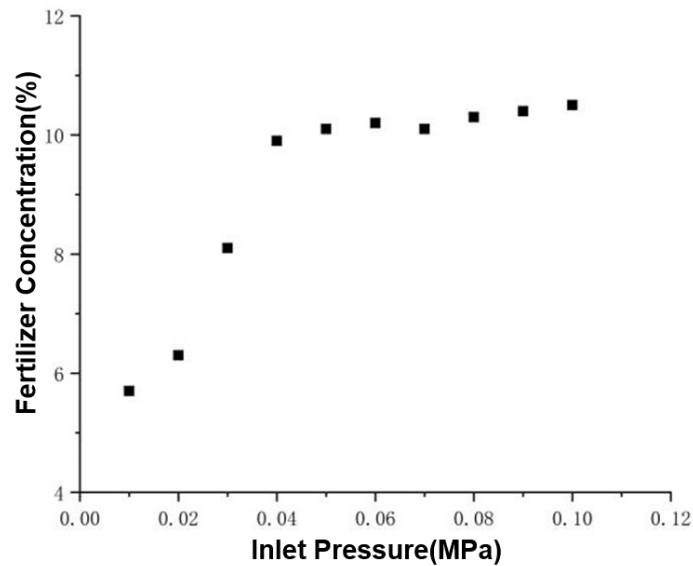


Fig. 13. Relationship between the fertilizer fluid concentration and the inlet pressure

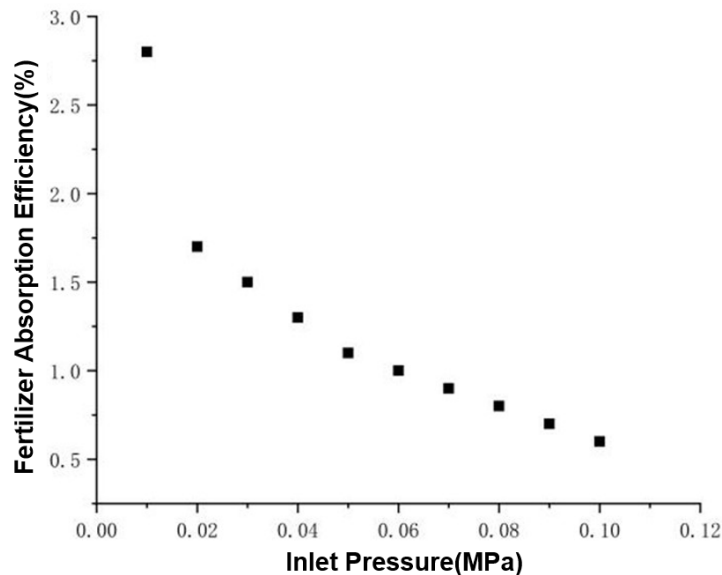


Fig. 14. Relationship between fertilizer efficiency and inlet pressure

As shown in Fig. 14, when the inlet pressure of the venturi fertilizer applicator varied within the range of 0.01 to 0.1 MPa, the fertilizer absorption efficiency of the venturi fertilizer applicator decreased from 2.8 to 0.6%. The results showed that when the outlet of the venturi fertilizer applicator was in the state of self-flowing, and the inlet pressure was 0.05 MPa, the efficiency of the fertilizer absorption was 1.1%, which can satisfy the actual demand.

## CONCLUSIONS

1. The maize variety Demeria D3 was the research object. Python language was used to write the deep learning framework of PyTorch. The recognition method of the growth period of maize plants was proposed based on the MobileNet model. The validity of the model was verified through the test set. Results showed that the maize plants in the seedling stage, the nodulation stage, the staminate stage, the milky ripening stage, and the completion stage were 98%, 96%, 92%, 85%, and 97%, respectively.
2. Based on the plant height measurements of maize plants in the experimental area at the seedling, nodulation, and stamen pulling stages, a comparative analysis of the prediction models before and after optimization was conducted by applying the Prophet model and the optimized Prophet model. Results showed that the predictive model of maize plant height was applicable and that the relative errors of the predicted values of the Prophet model were 0.85%, 2.11%, and 0.79%. The relative errors of Prophet optimization model were 0.76%, 0.47% and 0.71%. Compared to the Prophet model, the optimized errors were reduced by 0.09%, 1.64% and 0.08%.

## ACKNOWLEDGEMENTS

Heilongjiang Province Excellent Young Teachers Basic Research Support Program (YQJH2023218); Key Laboratory Open Topics of Field Agricultural Equipment Engineering Technology in Heilongjiang (TJNY202302); Basic Scientific Research Expenses Project of Universities in Heilongjiang Province (2023-KYYWF-0571); Science and Technology Plan Innovation incentive program of Jiamusi (NY2023JL0006); Heilongjiang Province Department of Education Science and Technology Innovation Team Construction Plan Project (2021-KYYWF-0639).

## REFERENCES CITED

- Cai, J., Chang, H., Chen, H., Zhang, B., Wei, Z., and Peng, Z. (2020). "Simulation of maize dry matter accumulation based on different effective accumulated temperatures," *Journal of Agricultural Machinery* 51(5), 263-271. DOI: 10.6041/j.issn.1000-1298.2020.05.029
- Chen, M., Yu, H., Li, X., Wang, H., Liu, S., Kong, L., Zhang, L., Dang, J., and Sui, Y. (2021). "Response analysis of hyperspectral characteristics of maize seedling leaves under different light and temperature environment," *Spectroscopy and Spectral Analysis* 41(11), 3545-3551.

- Chen, X. (2021). *Intelligent Monitoring System for Integrating Water and Fertilizer Based on the Internet of Things*, Master's Thesis, Tianjin University of Technology.
- Fan, X., Zhou, J., Xu, Y., Li, K., and Wen, D. (2021). "Identification and localization of weeds based on optimized Faster R-CNN in cotton seedling stage," *Journal of Agricultural Machinery* 52(5) 26-34. DOI: 10.6041/j.issn.1000-1298.2021.05.003
- GB 1353-2018 (2018). "National standards of the people's republic of China," Standards Press, Beijing, China.
- Gu, T. (2023). *Research on the Intelligent Identification Algorithm of Maize Growth State*, Master's Thesis, East China Normal University.
- Gupta, K., Rani, R., and Bahia, N. K. (2020). "Plant-seedling classification using transfer learning-based deep convolutional neural networks," *International Journal of Agricultural and Environmental Information Systems* 11(4), 25-40. DOI: 10.4018/IJAEIS.2020100102
- Huan, J., Li, D., Du, Y., Shen, X., Zhang, X., Qiao, B., He, C., Lan, X., and Luo, S. (2023). "Real-time load mid-term prediction based on Prophet algorithm and blending integrated learning," *Power Automation equipment*. DOI: 10.16081/j.epae.202308025
- Huang, S. (2023). *UAV-based Image Recognition of Maize Growth Period*, Master's Thesis, Jilin Agricultural University.
- Ikasari, I. H., Ayumi, V., Fanany, M. I., and Mulyono, S. (2016). "Multiple regularizations deep learning for paddy growth stages classification from LANDSAT-8," *International Conference on Advanced Computer Science and Information Systems (ICACSIS)* 512-517. DOI: 10.1109/ICACSIS.2016.7872790
- Lanlan, F., Hao, H., Heng, W., Shengcao, H. and Du, C. (2022). "Classification of maize growth stages using the Swin Transformer model," *Agricultural Engineering Journal* 38(14). DOI: 10.11975/j.issn.1002-6819.2022.14.022
- Liang, Q., Zhang, X., Ge, Y., and Chi, J. (2023). "I Quantitative seed supply prediction model of super rice," *China Agricultural Machinery Chemistry Journal* 44(8), 148-154.
- Li, Y. (2021). *Research on Classification and Recognition of Growing Period of Winter Wheat in Central China Plain Based on Deep Feature Learning and Multi-level R-CNN*, Master's Thesis, North China University of Water Resources and Electric Power. DOI: 10.27144/d.cnki.ghbsc.2021.000388
- Liu, R., Li, Y., Liu, Z., Liu, L., and Lu, H. (2021). "Analysis and calibration of discrete element parameter of coated maize seed," *Transactions of the Chinese Society for Agricultural Machinery* 52, 1-8. DOI: 10.6041/j.issn.1000-1298.2021.S0.001
- Ma, H., Dong, K., Wang, Y., Wei, S., Huang, W., and Gou, J. (2023). "Lightweight plant recognition model study based on improved YOLO v5s," *Journal of Agricultural Machinery* 54(8), 267-276. DOI: 10.6041/j.issn.1000-1298.2023.08.026
- Pan, G. (2022). *Research on Wood Tree Species Identification Based on Lightweight Convolutional Neural Network*, Master's Thesis, Fujian Agriculture and Forestry University. DOI: 10.27018/d.cnki.gfjnu.2022.000166
- Wang, D., and Wang, J. (2021). "Crop disease classification with transfer learning and residual networks," *Journal of Agricultural Engineering* 37(4), 199-207. DOI: 10.11975/j.issn.1002-6819.2021.4.024
- Xiong, J., Dai, S., District, J., Lin, X., Huang, Q., and Yang, Z. (2020). "Leaf deficiency symptoms detection method of soybean based on deep learning," *Journal of Agricultural Machinery* 51(1), 195-202. DOI: 10.6041/j.issn.1000-1298.2020.01.021

- Xu, J., Shao, M., Wang, Y., and Han, W. (2020). "Recognition of corn leaf spot and rust based on transfer learning with convolutional neural network," *Journal of Agricultural Machinery* 51(2), 230-236. DOI: 10.6041/j.issn.1000-1298.2020.02.025
- Xu, J., Wang, J., Xu, Xi., and Ju, S. (2021). "Image recognition for different developmental stages of rice by RAdam deep convolutional neural networks," *Journal of Agricultural Engineering* 37(8), 143-150. DOI: 10.11975/j.issn.1002-6819.2021.08.016
- Zhang, Y., Liu, R., Liu, M., and Gong, Y. (2018). "Maize growth period recognition based on deep convolution feature," *Electronic Measurement Technology* 41(16), 79-84. DOI: 10.19651/j.cnki.emt.1801669
- Zhang, J., and Li, J. (2019). "Experimental and analysis of Venturi injector fertilizer performance in low-pressure irrigation system," *Journal of Agricultural Mechanization Research* 41(2), 183-186. DOI: 10.13427/j.cnki.njyi.2019.02.034
- Zhao, C., Wen, C., Lin, S., Guo, W., and Long, J. (2020). Tomato florescence recognition and detection method based on the cascaded neural network," *Journal of Agricultural Engineering* 36(24), 143-152. DOI: 10.11975/j.issn.1002-6819.2020.24.017
- Zhao, L., Hou, F., Lu, Z., Zhu, H., and Ding, X. (2020). "Image recognition of cotton leaf diseases and pests based on transfer learning," *Journal of Agricultural Engineering* 36(7), 184-191. DOI: 10.11975/j.issn.1002-6819.2020.07.021
- Zheng, G., Wei, J., Ren, Y., Liu, H., and Xi, L. (2022). "Study on lightweight wheat growth process monitoring model based on depth separability convolution and dilated convolution," *Jiangsu Agricultural Science* 50(20), 226-232. DOI: 10.15889/j.issn.1002-1302.2022.20.034

Article submitted: March 11, 2024; Peer review completed: May 19, 2024; Revised version received: June 12, 2024; Accepted: June 13, 2024; Published: June 26, 2024. DOI: 10.15376/biores.19.3.5450-5466